



Contents lists available at ScienceDirect

Journal of Non-Crystalline Solids

journal homepage: www.elsevier.com/locate/jnoncrysolQuasi-static and impact-initiated response of $\text{Zr}_{55}\text{Ni}_5\text{Al}_{10}\text{Cu}_{30}$ alloy

Caimin Huang, Shun Li, Shuxin Bai*

Department of Materials Science and Engineering, National University of Defense Technology, Changsha, China

ARTICLE INFO

Keywords:

 $\text{Zr}_{55}\text{Ni}_5\text{Al}_{10}\text{Cu}_{30}$

Bulk metallic glass

Mechanical properties

Reactive material

ABSTRACT

The $\text{Zr}_{55}\text{Ni}_5\text{Al}_{10}\text{Cu}_{30}$ alloy was prepared by copper-mold casting method. The microstructure of the alloy was examined by integrating the X-ray diffraction, scanning electron microscope and electron probe microanalyzer. It was found that the alloy cast in the mold with 3 mm in diameter contains amorphous and $\text{Cu}_{10}\text{Zr}_7$ phases, while the alloys cast in the mold with 6 (D6) and 10 mm in diameter consist of $\text{Cu}_{10}\text{Zr}_7$, CuZr_2 crystalline and amorphous phases. The quasi-static experiment result shows that the compressive fracture strength of D6 is up to 1560 MPa. Moreover, it was found that the $\text{Zr}_{55}\text{Ni}_5\text{Al}_{10}\text{Cu}_{30}$ alloy burned completely in air based on the evolution of bright spark during ballistic impact testing. The obviously reaming effect to impact target indicates that the $\text{Zr}_{55}\text{Ni}_5\text{Al}_{10}\text{Cu}_{30}$ alloy has a promising application in reactive material.

1. Introduction

Zr-based bulk metallic glasses (BMGs) are known to have good glass forming ability and outstanding mechanical properties, including ultra-high strength, high hardness and large elastic limit [1–3]. However, monolithic Zr-based BMG usually suffers limited plasticity at room temperature. To understand the mechanism of the elasticity and plasticity of the BMGs, molecular dynamics simulations [4,5] and theoretical developments connecting macroscopic experimental response were reported previously [6]. It was reported that the formation of nanocrystallization and free volume is important for acquiring large strain in the Zr-based bulk metallic glasses [7,8]. Homogeneous distribution of fine crystalline phases in the matrix may also enhance the mechanical properties of the alloy [9–11]. In the Zr–Al–Ni–Cu BMG, some Zr-rich and Cu-rich crystalline phases, i.e. Zr_2Ni , Zr_2Cu , $\text{Zr}_7\text{Cu}_{10}$ and Zr_3Al , were found and discussed in previous works [12–14]. However, a further investigation on the interaction between second phase and extending shear band is quite necessary, and the effects of cooling rate on microstructure of the precipitates in the $\text{Zr}_{55}\text{Al}_{10}\text{Ni}_5\text{Cu}_{30}$ alloy have not been investigated in detail yet. Experimentally, it is not easy to accurately control the cooling rate of a given system. According to Lin et al. [15], the relationship between cooling rate and a sample of given dimension R can be expressed as

$$\dot{T} = \frac{K(T_m - T_t)}{CR^2} \quad (1)$$

where T_t is a given temperature, T_m initial cooling temperature ($T_m \geq T_t$), K is the thermal conductivity and C is the heat capacity per unit volume. Notice that when K , $T_m - T_t$ and C keep constant, one order

of magnitude increasing in the dimension R is equivalent to a two order of magnitude decrease in the cooling rate. In the present work, the cooling rate is estimated from the casting diameter of the alloys.

On the other hand, it was found that some metastable materials, like Zr-based bulk metallic glasses (BMGs), can also be served as reactive materials (RMs) [16–17]. Unlike traditional reactive material, Zr-based BMGs integrate desirable characteristics of high mechanical strength and energy density. Although they are inert under traditional initiation manner such as flame initiation cannot sustain a reaction, it will be triggered into reactions in case of the sufficient reaction driving energy supplied by hitting the targets with great velocity or intense dynamic loading [17]. As a result, the rapidly release energy significantly enhance the structure damage of the targets. Furthermore, the reaction between the fine fragments and oxygen can release a large of energy and rapidly burn in the air, which will produce second damage. However, there is little investigation on the impact initiation behavior of Zr-based alloys.

We selected the $\text{Zr}_{55}\text{Al}_{10}\text{Ni}_5\text{Cu}_{30}$ alloy as the focus of our study because it has large potential application for reactive material. The main objectives of the present work are: (i) to investigate the effect of cooling rate on the microstructure of precipitates in $\text{Zr}_{55}\text{Al}_{10}\text{Ni}_5\text{Cu}_{30}$ alloy using different as-cast rod in diameters; (ii) to study the effect of precipitates on the mechanical properties on the $\text{Zr}_{55}\text{Al}_{10}\text{Ni}_5\text{Cu}_{30}$ alloy by the means of uniaxial-compressive experiment; (iii) to investigate the impact initiation behaviors of the $\text{Zr}_{55}\text{Al}_{10}\text{Ni}_5\text{Cu}_{30}$ alloy by means of impact initiation.

* Corresponding author.

E-mail address: nudt_rms_501@163.com (S. Bai).<http://dx.doi.org/10.1016/j.jnoncrysol.2017.10.011>Received 30 July 2017; Received in revised form 1 October 2017; Accepted 12 October 2017
0022-3093/ © 2017 Elsevier B.V. All rights reserved.

2. Experimental procedures

High-purity elements of Zr (purity: 99.99 wt%), Cu (purity: 99.99 wt%), Ni (purity: 99.9 wt%), and Al (purity: 99.99 wt%) were purchased from Alfa Aesar (China) Chemicals Co., Ltd., and were used to prepare the $Zr_{55}Cu_{30}Ni_{15}Al_{10}$ alloy to minimize possible contamination by tracer elements. The master ingots with nominal compositions of $Zr_{55}Cu_{30}Ni_{15}Al_{10}$ were prepared by arc-melting under a argon atmosphere. To ensure chemical homogeneity, the ingots were turned over and remelted for four times. The cylindrical samples with 3, 6 and 10 mm in diameter (named as D3, D6 and D10 hereinafter, respectively) and 50 mm in height were obtained by remelting the master ingots in a vacuum quartz tube and injection-casting the melts into a water cooled copper mold.

All samples were subjected to microstructure observation. Specimens were taken at 10 mm from the bottom of the samples by wire-electrode cutting. Each specimen was mechanically ground and further polished on automatic polishing equipment using an oxide polishing suspension (OP-S) at a rotation speed of 400 rpm. The X-ray diffraction data of samples were collected on a Bruker D8 Advance (D8AA25X) powder diffractometer using Cu K α radiation ($\lambda = 1.5406 \text{ \AA}$). The diffractometer was operated at 40 kV and 40 mA, the 2θ scan ranges from 20 to 90° with a step size of 0.02 and a counting time of 0.5 s per step. The micrograph samples were examined and analyzed by back-scattered electron (BSE) (JXA-8530, JEOL, Japan) mode equipped within an electron probe microanalyzer (EPMA; JXA-8530, JEOL, Japan). The average area of the crystalline phase was measured by image analysis using an Image-Pro plus 6.0 metallographic analyzer.

The Compressive measurement at a quasi-static strain rate was performed on a universal testing machine (America instron-3369) with the strain rate of $0.5 \times 10^{-4}/s$. The aspect ratio of the sample is 1:1. For each sample, three specimens were tested and the mean value was accepted. The dynamic response of the alloy was tested using the ballistic impact method. The sample was embedded in a nylon sabot and then firmly inserted into a cartridge. The projectile was launched by a 12.7 mm calibre ballistic gun. The distance between the gun and target plate is 15 m. A high-speed camera with 6000 fps was used to capture the impact-induced initiation of the sample. The schematic illustration of impact-induced initiation experiment is shown in Fig. 1.

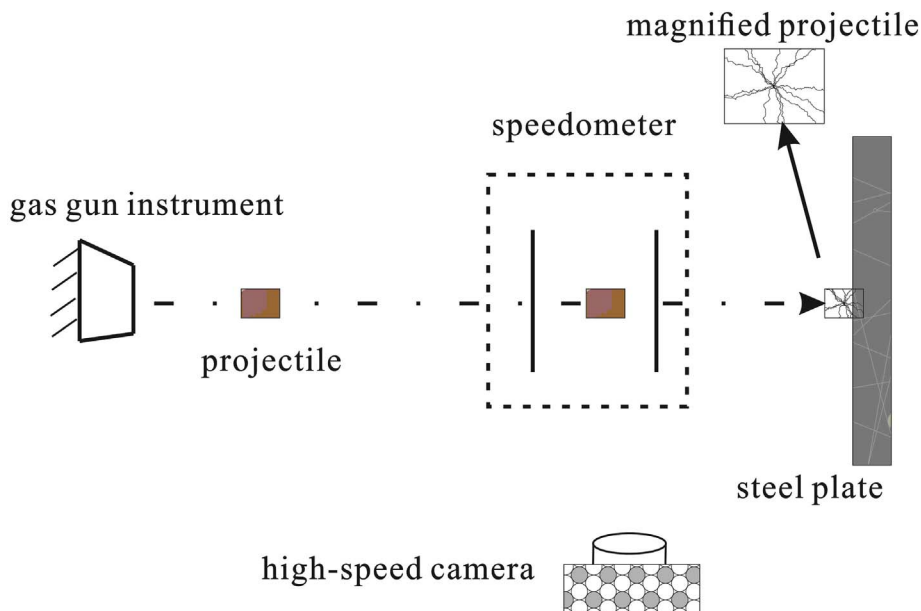


Fig. 1. The experimental setup for impact-induced tests.

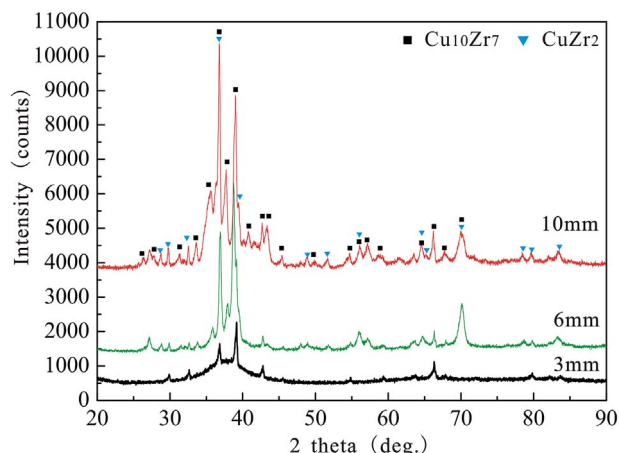


Fig. 2. XRD patterns of $Zr_{55}Cu_{30}Ni_{15}Al_{10}$ alloy with different casting diameters.

3. Results and discussion

3.1. Microstructure

Fig. 2 displays the XRD patterns of as-cast $Zr_{55}Cu_{30}Ni_{15}Al_{10}$ alloys taken from different cylindrical rods. As can be seen in the figure, the pattern of D3 consists of a clearly broad hump from 32° to 45° and several noticeable crystalline diffraction peaks that can be well indexed as $Cu_{10}Zr_7$ phase, indicating that the sample has a partial glassy structure. For the D6 specimen, besides the $Cu_{10}Zr_7$ crystallizing phase, a quasi-crystalline $CuZr_2$ was detected. Moreover, the peak intensity of $Cu_{10}Zr_7$ phase become stronger compared to the one in D3 sample. This suggests that more $Cu_{10}Zr_7$ crystalline phase appears in the alloy. As shown in the pattern of D10, a similar tendency as one in D6 can be observed, but the diffraction peaks corresponding to $CuZr_2$ phase become more intense in the D10 sample due to the increase of mold diameter. The quantitative analysis of XRD patterns of the alloys shows that the total volume fraction of crystalline phases is 49.46%, 68.65% and 82.17% for R3, R6 and R10 sample (see Fig. 3, shown only the pattern of R3 in here), respectively. This indicates that more crystalline phases occur with the increase of mold diameter.

The typical BSE images of various as-cast rods are shown in Fig. 4. From Fig. 4(a), it can be found that many dark contrast precipitates

Download English Version:

<https://daneshyari.com/en/article/7900235>

Download Persian Version:

<https://daneshyari.com/article/7900235>

[Daneshyari.com](https://daneshyari.com)